Applied Physics Letters ARTICLE pubs.aip.org/aip/apl

Iron dopant energy levels in β-Ga_2O_3

Cite as: Appl. Phys. Lett. **124**, 252104 (2024); doi: 10.1063/5.0213263
Submitted: 9 April 2024 · Accepted: 10 June 2024 ·
Published Online: 21 June 2024

Louis A. Angeloni,[1,a)] I.-J. Shan,[1] J. H. Leach,[2] and W. Andreas Schroeder[1]

AFFILIATIONS

[1]Department of Physics, University of Illinois Chicago, 845 W. Taylor St., Chicago, Illinois 60607, USA
[2]Kyma Technologies, Inc., 8829 Midway West Rd., Raleigh, North Carolina 27617, USA

[a)]Author to whom correspondence should be addressed: langel5@uic.edu

ABSTRACT

The energetic positions of the two Fe dopant levels in the bandgap of β-Ga_2O_3 are determined to be at 3.05(±0.05) and 3.85(±0.05) eV below the conduction band minimum from transmission measurements employing a sub-picosecond tunable ultraviolet laser radiation source. A further measurement of the quantum efficiency of photoelectron emission from the Fe:Ga_2O_3(010) photocathode is consistent with the obtained absorption data and a dominant optical phonon assisted Franck–Condon emission mechanism, while also providing an estimate of 100 ps for the conduction band electron lifetime.

The β crystalline form of gallium oxide (β-Ga_2O_3) is a material that has inspired significant development efforts due to its desirable electronic properties, among them a large bandgap energy (∼4.8 eV)[1] and high critical electric field,[2] combined with a potential to be cheaply produced at scale via methods like EFG (edge-defined film-fed growth).[3] The intended applications of this wide bandgap semiconductor commonly include high-power electronic[4] and optical devices,[5] the material being especially attractive in cases where radiation hardening is a concern.[6,7] Many such applications require semi-insulating material, which may be achieved through iron doping[8]—a *p*-type doping that depletes the ∼10^{16} cm^{-3} optically active and populated oxygen vacancy states in the bandgap[9] to produce a crystal transparent in the 400–700 nm (1.8–3.0 eV) visible spectral region. The exact energetic positions of the two expected Fe dopant states are, however, the subject of some debate in the literature: (i) Ingebrigtsen *et al.*[10] in their deep level transient spectroscopy (DLTS) measurements of *n*-type Ga_2O_3 materials reported an energy of 0.78 eV below the conduction band (CB) minimum and also suggested the existence of a Fe state ∼0.5 eV above the valence band (VB) maximum, while (ii) Lyons[11] indicated, citing Ref. 10, that the Fe dopant states are expected to be in the energetic vicinity of the deep acceptor Ca dopant states at 0.7–1.5 eV above the VB maximum. Accordingly, an accurate determination of the Fe energy levels in β-Ga_2O_3 at the ∼10^{18} cm^{-3} dopant densities employed to achieve semi-insulating behavior is of direct interest for *ab initio* acceptor state modeling[11,12] and clearly of relevance for device design due to the consequent likely Fermi level pinning at the dopant state energy. Recent reports[13–15] of shallow acceptor *p*-type doping could then complete the practical requirements for β-Ga_2O_3 based optical and electronic device design.

In this Letter, we present two separate experimental measurements into the properties of a Fe doped β-Ga_2O_3(010) crystal provided by Kyma Technologies, Inc.[16] The first is based on a standard spectral absorption measurement technique, albeit using a tunable sub-picosecond ultraviolet (UV) laser radiation source, which reveals the energetic positions of the two iron dopant states. The second employs a low energy photoemission measurement with the same UV laser system for which the quantum efficiency (QE) of electron emission is dependent upon the photoexcitation into and electron transport dynamics in the oxide's conduction band. The measured spectral dependence of the QE (in the studied ultrafast regime) is shown to be consistent with photoexcitation from the Fe dopant states at their determined energetic positions in the oxide's bandgap and subsequent emission into the vacuum through an optical phonon mediated Franck–Condon mechanism.[17–19]

The studied 450(±50) μm-thick β-Ga_2O_3(010) material is semi-insulating due to ∼10^{18} cm^{-3} iron doping. The wide-gap semiconductor wafer is colorless and has an epi-ready front surface finish (RMS roughness <0.5 nm) with the back surface polished to optical quality (better than $\lambda/4$ at 632 nm). The transparency of the oxide wafer over the visible spectrum (1.8–3.0 eV) indicates that the Fermi level is almost certainly pinned at least 3 eV below the CB minimum and very likely at a Fe dopant state due to the moderately high dopant density. Consequently, optical transitions into the CB from the VB, occupied Fe dopant states, and perhaps oxygen vacancy states[9] below the Fermi level

are only possible at near UV (and shorter) wavelengths (i.e., $\hbar\omega$ >3.0 eV). The presented experimental measurement techniques employ sub-picosecond (~0.5 ps) UV pulses tunable from 230 to 400 nm (3.0–5.3 eV) that have a typical pulse energy of ~10 pJ. The UV pulses are generated using a 16.7 MHz repetition rate laser-based radiation source driven by a 20 W Yb:fiber laser system (aeroPULSE FS20; NKT Photonics) producing ~350 fs duration laser pulses at 1030 nm.[20,21]

For the spectral absorption measurements of the uncoated Fe:Ga_2O_3(010) wafer, the incident UV laser beam is collimated to a diameter of ~2 mm, giving a peak pulse intensity of less than 1 kW/cm^2, and the transmission determined as a function of the incident photon energy $\hbar\omega$ for radiation at near normal incidence (i.e., angle of incidence < 5°). The results, shown as the black data points in Fig. 1, include the second harmonic of the Yb:fiber laser system at 515 nm ($\hbar\omega = 2.4$ eV). They clearly indicate a transmission of ~70% in the visible ($\lambda > 400$ nm), primarily due to loss by surface reflections, and an increasing absorption to near zero (<0.1%) transmission for $\hbar\omega$ > 4.6 eV. The latter value is slightly less than the expected bandgap energy of 4.8 eV (Ref. 1) due to either a strong Urbach absorption tail[22] or transitions from the VB to a higher density of oxygen vacancy states in the vicinity of the CB.[9] We note that interference effects from multiple surface reflections are minimized (if not effectively eliminated) using the ~0.5 ps pulses in the transmission measurements since the ~150 μm spatial pulse length is significantly less than the $2nl \approx 2$ mm optical thickness of the wafer (assuming a refractive index $n \approx 2$[23] and a thickness of $l = 450$ μm).

For the spectral photoemission measurements, a ~7 × 7 mm^2 portion of the Fe:Ga_2O_3 wafer is mounted in the cathode of a 16 kV DC electron gun based on the design of Togawa *et al.*[24] The tunable and *p*-polarized UV pulsed laser radiation at a 60° angle of incidence is focused to an elliptical 35 × 70 μm^2 (half-width at half irradiance maximum) Gaussian spot on the Ga_2O_3 photocathode. After acceleration across the 1 cm DC gun length, the photoemitted electrons are incident on a micro-channel plate (MCP) detector with a P43 phosphor screen (BOS-18; Beam Imaging Solutions). The resultant optical signal due to the electron beam is then relay imaged onto a 2.5 μm pixel CMOS camera. The sensitivity of the MCP/camera system is calibrated against the known electron photoemission quantum efficiency (QE) of a Rh(110) photocathode whose spectral QE dependence has been determined using a Faraday cup.[20] The integrated camera image of the electron beam and the incident UV laser power can then be directly related to the QE of the Ga_2O_3 photocathode once the transmission of the UV fused silica vacuum window and reflectivity of the front surface of Ga_2O_3 crystal are accounted for. The latter is minimal (less than 1%) for our *p*-polarized 230–400 nm radiation since the tangent of the 60° angle of incidence is close to the refractive index of Ga_2O_3.[23] The spectral dependence of the QE for our Fe:Ga_2O_3 photocathode measured in this manner is plotted as the square root of the QE vs the incident photon energy $\hbar\omega$ in Fig. 2.

We note that the incident laser irradiances of less than 100 kW/cm^2 employed in both measurements are expected to be significantly less than those required to observe nonlinear optical effects. For Ga_2O_3 with its 4.8 eV bandgap, the band to band two-photon absorption coefficient is expected to be ~1 cm/GW (Refs. 25 and 26) so that for the 450 μm-thick wafer, a two-photon absorption of 1% would require an incident laser pulse intensity of at least 1 MW/cm^2. Further, the birefringence of Ga_2O_3 is not expected to play a major role in both sets of measurements since the (010) wafer orientation places the most dissimilar optical axis[1] closest to the direction of propagation of the UV radiation.

Without interference effects, the irradiance transmission T through an uncoated absorbing material of thickness l is given in general by

$$T = (1 - R)^2 S e^{-\alpha l}, \tag{1}$$

where R is the reflectivity of each face, α is the optical absorption coefficient, and S is an additional loss term accounting for scattering

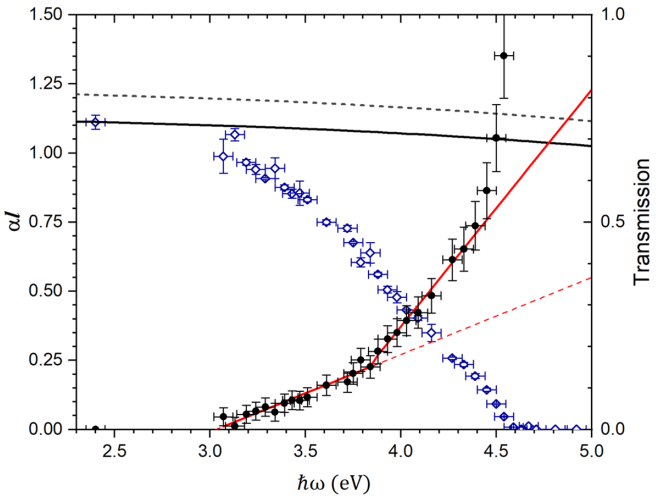

FIG. 1. Spectral dependence of the transmission (right axis) and αl (left axis) for the Fe:Ga_2O_3(010) wafer: experimental transmission (open blue circles), $(1 - R)^2$ using refractive index of Ref. 17 (dashed black line), $(1 - R)^2 S$ with $S = 0.919$ (solid black line), and extracted values of αl (black points) and their fit to two linear functions (solid and dashed red lines).

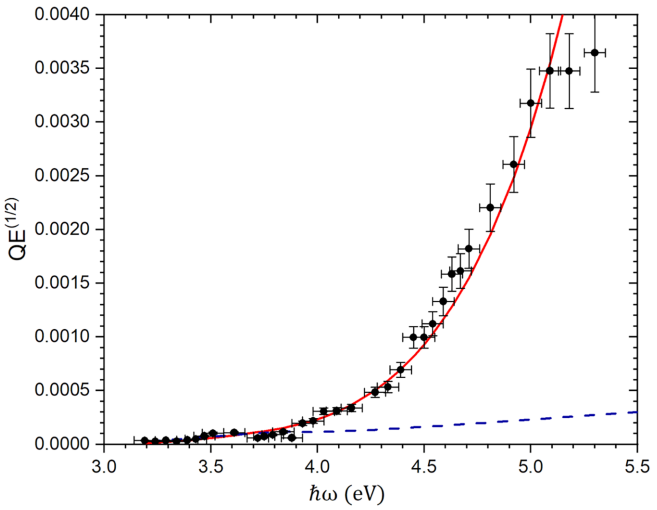

FIG. 2. Spectral dependence of the square root of the QE for Fe:Ga_2O_3(010): fit for $\hbar\omega < 3.8$ eV using Eq. (3) (dashed blue line) and fit for $\hbar\omega < 4.8$ eV using Eq. (4) (solid red line).

effects, background absorption (e.g., from the valence band to unoccupied oxygen vacancy states in the bandgap), etc. This relation is used to evaluate αl using the measured transmission data displayed as the black data points in Fig. 1. Under our conditions of normal incidence and assuming a negligible imaginary component to the refractive index, the reflection of each surface is $R = \left(\frac{n-1}{n+1}\right)^2$ for a (real) refractive index n. The resulting spectral dependence of $(1-R)^2$ using the dispersion of the refractive index determined by Rebien *et al.*[23] is plotted as the black dashed line in Fig. 1. Incorporating a value of $S = 0.919$ to fit the value of $(1-R)^2 = 0.741$ measured at $\hbar\omega = 2.4$ eV (the second harmonic of the Yb:fiber laser at 515 nm) produces the solid black line. Evaluation of αl for each experimental data point using Eq. (1) generates the red points plotted in Fig. 1. The spectral trend of $\alpha(\hbar\omega)l$ below $\hbar\omega \approx 4.4$ eV can be well fit by the addition of two linear dependences of the form $A_i(\hbar\omega - E_i)$, valid for $\hbar\omega > E_i$, where A_i is a constant and E_i is a threshold energy. This fit is shown by the solid red line in Fig. 1 for $E_1 = 3.05$ eV and $E_2 = 3.85$ eV.

A linear increase in the absorption with incident photon energy $\hbar\omega$ from a threshold energy is consistent with expectations for transitions from an atomic-like dopant state to an unpopulated CB centered on the Γ point of the Brillouin zone. In the limit of an energetically narrow dopant state with a constant density of states (i.e., a momentum width significantly larger than the momentum of the excited state in the CB), an evaluation of the absorption through the joint density of states associated with the optical transition reduces to an integral of the form,

$$\alpha_i \propto \int_0^\infty p^2 dp\, \delta\left(p - \sqrt{2m^*(\hbar\omega - E_i)}\right) = 2m^*(\hbar\omega - E_i), \quad (2)$$

where the delta function (Fermi's golden rule) defines energy conservation in the optical transition. Here, both the dopant state and CB with an effective mass m^* are assumed to be isotropic in momentum space, and E_i is the energy of the dopant state below the CB minimum. The observed threshold energies E_1 and E_2 in Fig. 1 can therefore now be identified as the energetic positions of the two Fe dopant states in Fe:Ga_2O_3. Also of note is that the fitted values of A_1 and A_2 are comparable ($A_2 = 2.07A_1$), implying that the product of the absorption cross sections and occupied state density for the two Fe states is also comparable—the observation that A_2 is greater than A_1 by a factor of 2 may simply be due to the upper Fe dopant state pining the Fermi level.

Under our experimental conditions with 3.0–5.3 eV incident UV photon energies, the observation of photoemission from Fe:Ga_2O_3 when $\hbar\omega < 4$ eV (Fig. 2) is perhaps somewhat surprising since our density functional theory (DFT) calculations (using the Amsterdam Suite[27] and the thin slab technique[28]) indicate that the vacuum level is 1 to 1.5 eV above the CB minimum. These calculations employ the rSCAN functional[29] with an undoped semi-slab of $2n$ atomic layers (with a clean un-passivated surface) and an "infinite" vacuum and are terminated for increasing n when both the energetic position of the VB maximum in the slab and the vacuum energy level converge to ±50 meV, giving a typical ±0.1 eV computational uncertainty in the work function. For the complex monoclinic crystal structure of β-Ga_2O_3, this energy convergence is more difficult to attain, leading to a larger work function uncertainty. Nonetheless, for conventional one-photon photoemission from this p-type doped wide-gap semiconductor where the Fermi level is pinned ∼1 eV above the VB maximum (i.e., greater than 3 eV below the CB minimum), our work function calculations indicate that a photon energy greater than 4 eV should be required. However, our experiments are performed using sub-picosecond laser pulses, which require ultrafast effects to be considered. In particular, the photoexcitation of "hot" electrons into the CB with an excess energy $\Delta E = \hbar\omega - E_i$, where E_i is the internal ionization energy of the ith dopant (or defect) state in the material's bandgap, will initially generate an electron distribution with a temperature T_e given by $k_B T_e = \frac{2}{3}\Delta E$, where k_B is Boltzmann's constant. In crystals, like Ga_2O_3, with a strong coupling between electrons and optical phonons, the initial temperature of the electron distribution is further reduced by energy equipartition with the optical phonon modes.[30,31] Thereafter, the transport dynamics of the electrons under the applied field in the Fe:Ga_2O_3(010) crystal, due to the 16 MV/cm acceleration field in the DC gun, determine the temperature of the electron distribution as it approaches the crystal emission face. In the non-degenerate photoexcitation limit, which is applicable under our experimental conditions, this means that a small fraction of the electrons in the high energy portion of the population tail in their Boltzmann distribution will have sufficient energy to overcome the ∼1 eV potential barrier to be emitted into the vacuum from the CB.

The QE of this photoemission mechanism has been shown to be proportional to the square of the initial excited carrier energy ΔE in the CB;[30] fundamentally, this is because (i) the fraction of electrons in the CB above the ≥1 eV emission barrier is proportional to T_e and (ii) the emission probability into the vacuum is the product of the transmission coefficient for the potential barrier and the density of the recipient vacuum states (both being proportional to the square root of the emission energy in the vacuum). For the two optically active Fe dopant states in Ga_2O_3 with internal ionization energies E_1 and E_2, the square root of the photoemission QE is therefore expected to be of the following form:

$$\sqrt{QE} \propto k_B T_e = B\left[\frac{A_1(\hbar\omega - E_1)^2 + A_2(\hbar\omega - E_2)^2}{A_1(\hbar\omega - E_1) + A_2(\hbar\omega - E_2)}\right], \quad (3)$$

where B is a constant and from the transmission data analysis $A_2/A_1 = 2.07$. As shown by the blue dashed line in Fig. 2, this form for the spectral dependence of the QE is clearly not consistent with the experimental data when $E_1 = 3.05$ eV and $E_2 = 3.85$ eV; Eq. (3) can only be fit to the QE data below $\hbar\omega \approx 3.9$ eV.

A more sophisticated fit, which is consistent with the measured spectral QE data, is shown by the red line in Fig. 2. It is given by the following expression:

$$QE = C\{1 - e^{-\alpha l}\}\left\{\left[\frac{\alpha(1 - e^{-(\alpha+\beta)l})}{(\alpha+\beta)(1 - e^{-\alpha l})}\right]^9\right\}(k_B T_e)^2, \quad (4)$$

where C is a constant [not equal to B in Eq. (3)] and $k_B T_e$ is given by Eq. (3). The first term in the brackets reflects the modification required to correctly model the absorbed UV radiation over the 450 μm Fe:Ga_2O_3 wafer thickness since the QE can only be due to photoexcited electrons. The second bracketed term deals with the fraction of the photoexcited electrons that can be emitted from an escape depth $\beta^{-1} = v\tau$ associated with the electron drift velocity v to the emission face due to the applied field in the DC gun and recombination (presumably primarily into the empty oxygen vacancy states) in a

characteristic time τ; that is, it deals with the physics of the second transport step in Spicer's three-step photoemission model.[32] This fraction is raised to a power $k+1=9$, which is reflective of the physics of the electron emission mechanism into the vacuum.

For Ga_2O_3, we observe the dominant electron emission process to be due to a momentum resonant Franck–Condon effect[17–19] based on optical phonon scattering. A similar emission process has also been observed from a H-terminated diamond (001) surface,[33] where an average of two phonon scattering (emission) events occurs for every emitted electron. Due to its strong ionic nature and monoclinic crystal structure, Ga_2O_3 has many more (~5–6) strong and active optical phonon modes ranging in energy from ~100 meV to below $k_BT_L=25$ meV (Ref. 34) (where T_L is the 300 K lattice temperature). Consequently, it is probable that several (perhaps as many as 6–10, reflective of ~2 per mode) optical phonon scattering events could be involved in a single electron emission from this oxide material. Further, as the phonon population is generated by the electron distribution as it drifts toward the (010) emission face under the applied field,[31] it is reasonable to expect its spatial distribution (in the emission direction) to mimic closely that of the electrons. Hence, the square bracketed fraction of photoexcited electrons within the escape depth in Eq. (4) is raised to the power $k+1$ for k phonon scattering events plus the original electron distribution. The best fit of Eq. (4) to the spectral QE data (red line in Fig. 2) is obtained for $k=8$ and $\beta l=15$, with uncertainties of ±10% for both quantities. The fit also explicitly uses the spectral values of αl obtained from our transmission measurements; that is, the extracted values of E_1 and E_2 for the energies of the Fe dopant states and their relative absorption strengths $A_2/A_1=2.07$. The fit is good even between 4.4 and 4.8 eV, supporting the notion that the additional absorbance noted in this spectral region (Fig. 1) is likely due to transitions from the valence band into empty oxygen vacancy states just below the conduction band[9]—generating trapped electrons that cannot contribute to photoemission. Beyond 4.8 eV, the fit overestimates the QE since direct band to band transitions are now possible, thereby exciting many more electrons into the conduction band but with a much-reduced excess energy and therefore significantly decreasing the total energy k_BT_e of the photoexcited electron distribution. We also note that although the employed theoretical interpretation is consistent with the measured spectral QE trend below 4.8 eV, it cannot be considered exact as it does not account for all possible photoexcitation mechanisms such as those from occupied oxygen vacancy states between the two Fe states.[9]

If one assumes that the electrons are accelerated to the emission surface to a limiting average energy of $k_BT_D=62$ meV,[35] where T_D is the Debye temperature, before energy relaxation in the conduction band by optical phonon emission, then the obtained 30(±5) μm value of the electron escape depth β^{-1} can be used to estimate the electron lifetime τ in the conduction band of our Fe:Ga_2O_3 material. Specifically, $\frac{1}{2}m^*v^2=k_BT_D$ with $m^*=0.2$–$0.25m_e$ for the conduction band effective mass[1] (m_e is the free electron mass) gives an average electron drift velocity of $v\approx 3\times10^5$ m/s and hence $\tau=(v\beta)^{-1}\approx 100$ ps. This value for the CB electron lifetime is quite reasonable considering the anticipated ~10^{16} cm^{-3} density of available unpopulated oxygen vacancy states in the oxide bandgap[9] produced by the iron doping pinning the Fermi level ~3 eV below the CBM (i.e., at the upper Fe dopant state energy).[36]

The properties of an iron doped β-Ga_2O_3(010) crystal wafer have been investigated using two experimental techniques employing a sub-picosecond tunable UV laser system: (i) a standard spectral transmission measurement and (ii) a measurement of the spectral dependence of the QE of photoemission. The analysis of the UV transmission data indicates the presence of two Fe dopant states located 3.05(±0.05) and 3.85(±0.05) eV below the CB minimum—values that are consistent with *Ab initio* calculations of other deep acceptor dopant states in β-Ga_2O_3.[11,12] At the ~10^{18} cm^{-3} Fe dopant density, the observed photoemission threshold of 3.1(±0.1) eV for our ultrafast (sub-ps) measurement strongly suggests that the Fermi level is indeed pinned at the upper Fe dopant state—in agreement with visible optical clarity of the Fe:Ga_2O_3 wafer. The measured spectral dependence of the QE of photoemission is also shown to be consistent with emission from the high energy tail of a hot thermalized electron distribution generated by photoexcitation into the CB from the Fe dopant states, if recombination effects are included and a dominant Franck–Condon emission mechanism involving optical phonon scattering is assumed. The inclusion of the former allows for an estimate of 100 ps to be made for the electron lifetime in the CB of our Fe:Ga_2O_3 sample under the assumption that the electron energy gained in the applied DC gun field is limited to k_BT_D—the energy at the Debye temperature. The assumption of the latter momentum resonant electron emission mechanism is consistent with the expected strong optical deformation potential scattering in β-Ga_2O_3(010) and has been observed in prior studies of a H-terminated diamond (001) photocathode.[33]

This work was supported by the U.S. Department of Energy under Award No. DE-SC0020387. The authors gratefully acknowledge the expert assistance of the Liberal Arts and Sciences Machine Shop at the University of Illinois at Chicago.

AUTHOR DECLARATIONS

Conflict of Interest

The authors have no conflicts to disclose.

Author Contributions

Louis A. Angeloni: Conceptualization (equal); Data curation (lead); Formal analysis (lead); Investigation (equal); Software (lead); Visualization (lead); Writing – original draft (supporting); Writing – review & editing (equal). **I.-J. Shan:** Conceptualization (supporting); Data curation (supporting); Formal analysis (supporting); Writing – review & editing (equal). **J. H. Leach:** Resources (lead); Writing – review & editing (equal). **W. Andreas Schroeder:** Conceptualization (equal); Funding acquisition (lead); Project administration (lead); Supervision (lead); Writing – original draft (lead).

DATA AVAILABILITY

The data that support the findings of this study are available from the corresponding author upon reasonable request.

REFERENCES

[1]J. Zhang, J. Shi, D.-C. Qi *et al.*, "Recent progress on the electronic structure, defect, and doping properties of Ga_2O_3," APL Mater. **8**, 020906 (2020).
[2]E. Chikoidze, T. Tchelidze, C. Sartel, Z. Chi, R. Kabouche, I. Madaci, C. Rubio, H. Mohamed, V. Sallet, F. Medjdoub, A. Perez-Tomas, and Y. Dumont, "Ultra-high critical electric field of 13.2 MV/cm for Zn-doped p-type β-Ga_2O_3," Mater. Today Phys. **15**, 100263 (2020).

[3]K. N. Heinselman, D. Haven, A. Zakutayev, and S. B. Reese, "Projected cost of gallium oxide wafers from edge-defined film-fed crystal growth," Cryst. Growth Des. **22**(8), 4854–4863 (2022).
[4]A. J. Green, J. Speck, G. Xing, P. Moens, F. Allerstam, K. Gumaelius, T. Neyer, A. Arias-Purdue, V. Mehrotra, A. Kuramata, K. Sasaki, S. Watanabe, K. Koshi, J. Blevins, O. Bierwagen, S. Krishnamoorthy, K. Leedy, A. R. Arehart, A. T. Neal, S. Mou, S. A. Ringel, A. Kumar, A. Sharma, K. Ghosh, U. Singisetti, W. Li, K. Chabak, K. Liddy, A. Islam, S. Rajan, S. Graham, S. Choi, Z. Cheng, and M. Higashiwaki, "β-gallium oxide power electronics," APL Mater. **10**(2), 029201 (2022).
[5]H. Deng, K. J. Leedle, Y. Miao, D. S. Black, K. E. Urbanek, J. McNeur, M. Kozák, A. Ceballos, P. Hommelhoff, O. Solgaard, R. L. Byer, and J. S. Harris, "Gallium oxide for high-power optical applications," Adv. Opt. Mater. **8**, 1901522 (2020).
[6]D. A. Bauman, A. I. Borodkin, A. A. Petrenko, D. I. Panov, A. V. Kremleva, V. A. Spiridonov, D. A. Zakgeim, M. V. Silnikov, M. A. Odnoblyudov, A. E. Romanov, and V. E. Bougrov, "On improving the radiation resistance of gallium oxide for space applications," Acta Astronaut. **180**, 125–129 (2021).
[7]J. D. Blevins, K. Stevens, A. Lindsey, G. Foundos, and L. Sande, "Development of large diameter semi-insulating gallium oxide (Ga_2O_3) substrates," IEEE Trans. Semicond. Manuf. **32**(4), 466–472 (2019).
[8]S. Yu, Y. Liu, X. Hou, M. Ding, Y. Zou, Y. Guan, Z. Wu, X. Zhao, Q. Hu, G. Xu, and S. Long, "Stable Ga_2O_3 soft x-ray detector with ultrahigh responsivity," Appl. Phys. Lett. **124**, 181111 (2024).
[9]Z. Zhang, E. Farzana, A. R. Arehart, and S. A. Ringel, "Deep level defects throughout the bandgap of (010) β-Ga_2O_3 detected by optically and thermally stimulated defect spectroscopy," Appl. Phys. Lett. **108**, 052105 (2016).
[10]M. E. Ingebrigtsen, J. B. Varley, A. Yu. Kuznetsov, B. G. Svensson, G. Alfieri, A. Mihaila, U. Badstübner, and L. Vines, "Iron and intrinsic deep level states in Ga_2O_3," Appl. Phys. Lett. **112**, 042104 (2018).
[11]J. L. Lyons, "A survey of acceptor dopants for β-Ga_2O_3," Semicond. Sci. Technol. **33**, 05LT02 (2018).
[12]A. Kyrtsos, M. Matsubara, and E. Bellotti, "On the feasibility of p-type Ga_2O_3," Appl. Phys. Lett. **112**, 032108 (2018).
[13]M. M. Islam, M. O. Liedke, D. Winarski, M. Butterling, A. Wagner, P. Hosemann, Y. Wang, B. Uberuaga, and F. A. Selim, "Chemical manipulation of hydrogen induced high p-type and n-type conductivity in Ga_2O_3," Sci. Rep. **10**, 6134 (2020).
[14]J. Ma, J. Lin, J. Liu, F. Li, Y. Liu, and G. Yang, "Achieving high conductivity p-type Ga_2O_3 through Al-N and In-N co-doping," Chem. Phys. Lett. **746**, 137308 (2020).
[15]C. Ma, Z. Wu, H. Zhang, and H. Zhu, "P-type nitrogen-doped β-Ga_2O_3: The role of stable shallow acceptor N_O-V_{Ga} complexes," Phys. Chem. Chem. Phys. **25**, 13766 (2023).
[16]See www.kymatech.com for information on their Gallium oxide epiwafers.
[17]J. Franck, "Elementary processes of photochemical reactions," Trans. Faraday Soc. **21**, 536 (1926).
[18]E. Condon, "A theory of intensity distribution in band systems," Phys. Rev. **28**, 1182 (1926).
[19]P. Salek, F. Gel'mukhanov, H. Ågren, O. Björneholm, and S. Svensson, "Generalized Franck-Condon principle for resonant photoemission," Phys. Rev. A **60**, 2786 (1999).
[20]G. Adhikari, P. Riley, and W. A. Schroeder, "Spectral characterization of a Rh (110) photocathode: Band structure interpretation," AIP Adv. **9**, 065305 (2019).
[21]L. Angeloni, I.-J. Shan, and W. A. Schroeder, "Sub-threshold ultrafast one-photon photoemission from a Cu(111) photocathode," AIP Adv. **12**, 105129 (2022).
[22]D. Thapa, J. Lapp, I. Lukman, and L. Bergman, "Ultra-wide bandgap β-Ga_2O_3 films: Optical, phonon, and temperature response properties," AIP Adv. **11**, 125022 (2021).
[23]M. Rebien, W. Henrion, M. Hong, J. P. Mannaerts, and M. Fleischer, "Optical properties of gallium oxide thin films," Appl. Phys. Lett. **81**, 250 (2002).
[24]K. Togawa, T. Shintake, T. Inagaki, K. Onoe, and T. Tanaka, "CeB_6 electron gun for low-emittance injector," Phys. Rev. Spec. Top.-Accel. Beams **10**, 020703 (2007).
[25]M. Sheik-Bahae, D. J. Hagan, and E. W. Van Stryland, "Dispersion and band-gap scaling of the electronic Kerr effect in solids associated with two-photon absorption," Phys. Rev. Lett. **65**, 96 (1990).
[26]Y. Sun, Y. Fang, Z. Li, J. Yang, X. Wu, J. Jia, K. Liu, L. Chen, and Y. Song, "Ultrafast dynamics of optical nonlinearities in β-Ga2O3," Front. Mater. **8**, 754842 (2021).
[27]See http://www.scm.com for "Theoretical Chemistry" (SCM, Vrije Universiteit, Amsterdam, The Netherlands); G. te Velde and E. J. Baerends, "Precise density-functional method for periodic structures," Phys. Rev. B **44**, 7888 (1991); E. S. Kadantsev, R. Klooster, P. L. de Boeij, and T. Ziegler, "The formulation and implementation of analytic energy gradients for periodic density functional calculations with STO/NAO Bloch basis set," Mol. Phys. **105**, 2583 (2007).
[28]C. J. Fall, N. Binggeli, and A. Baldereschi, "Deriving accurate work functions from thin-slab calculations," J. Phys.: Condens. Matter **11**, 2689 (1999).
[29]A. P. Bartók and J. R. Yates, "Regularized SCAN functional," J. Chem. Phys. **150**(16), 161101 (2019).
[30]L. A. Angeloni, S. V. Baryshev, M. Mühle, and W. A. Schroeder, "Spectral emission properties of a nitrogen-doped diamond (001) photocathode: Hot electron transport and transverse momentum filtering," Phys. Rev. B **107**, 165105 (2023).
[31]K. Seeger, *Semiconductor Physics: An Introduction*, Springer Series in Solid-State Sciences Vol. 40 (Springer-Verlag, Berlin/Heidelberg/New York, 2004).
[32]W. E. Spicer, "Photemissive, photoconductive, and optical absorption studies of alkali-antimony compounds," Phys. Rev. **112**, 114 (1958).
[33]J. D. Rameau, J. Smedley, E. M. Muller, T. E. Kidd, and P. D. Johnson, "Properties of hydrogen terminated diamond as a photocathode," Phys. Rev. Lett. **106**, 137602 (2011).
[34]B. M. Jensen, R. Gillen, Z. Galazka, J. Maultzsch, and M. R. Wagner, "First- and second-order Raman spectroscopy of monoclinic β-Ga_2O_3," Phys. Rev. Mater. **6**, 054601 (2022).
[35]Z. Guo, A. Verma, F. Sun, A. Hickman, T. Masui, A. Kuramata, M. Higashiwaki, D. Jena, and T. Luo, "Anisotropic thermal conductivity in single crystal β-gallium oxide," Appl. Phys. Lett. **106**, 111909 (2015).
[36]O. Koksal, N. Tanen, D. Jena, H. Xing, and F. Rana, "Measurement of the ultrafast dynamic of photoexcited carriers in β-Ga_2O_3 by two-color optical pump-probe spectroscopy," Appl. Phys. Lett. **113**, 252102 (2018).